Lambda polarization at COMPASS

A. Ferrero

Dipartimento di Fisica Generale "A. Avogadro" and INFN - Torino, Italy

On behalf of the COMPASS collaboration

Abstract

New data on Λ^0 polarisation in semi-inclusive deep inelastic scattering have been collected by the COMPASS collaboration at CERN, using a beam of longitudinally polarised muons with an energy of 160 GeV. The Λ polarisation was measured through the weak decay $\Lambda \to p\pi^-$. First preliminary results on longitudinal and transverse Λ^0 polarization will be presented. Instrumental acceptance effects on the measured polarization will be discussed comparing real data and Monte Carlo simulations.

1 Introduction

The production of Λ^0 hyperons in polarized Deep Inelastic Scattering (DIS) is a powerful tool to provide new informations on the spin-dependent quark distributions inside the nucleon and the fragmentation process of quarks. The Λ^0 hyperons represent an unique tool to study polarization effects, since they act as natural polarimeters through their weak decay $\Lambda^0 \to p\pi^-$.

The results of Deep Inelastic Scattering experiments (see [1] and references therein for a review) suggest that the strange sea quarks may be negatively polarized with respect to the parent nucleon. This result can be verified by looking at the polarization transfer from longitudinally polarized nucleons to the Λ^0 produced in the target fragmentation region. The polarized intrinsic strangeness model[2, 3] predicts that the produced Λ^0 have a spin anti-correlated with that of the incoming lepton. The negative polarization has been confirmed by the NOMAD experiment[4] in the case of neutrino DIS.

The Λ^0 produced in the current fragmentation region can provide important informations on the spin-dependence of the fragmentation of quarks into hadrons. The idea behind the measurement is that a beam of longitudinally polarized leptons will preferentially strike quarks with a spin orientation parallel to that of the lepton. The quark polarization may then be transferred to the final state hadron through the fragmentation process. The longitudinal polarization transferred to the directly produced Λ^0's can be generally expressed, in the case of longitudinally polarized beam and unpolarized target nucleons, as[5]

$$P^{(+,0)}(x,y,z) = \frac{\sum_q e_q^2 q(x) \Delta D_{\Lambda/q}(z)}{\sum_q e_q^2 q(x) D_{\Lambda/q}(z)} \hat{A}_{LL}(y), \tag{1}$$

where the superscript denotes the lepton (+) and nucleon (0) polarizations, $q(x)$ is the number density of quarks of flavour q in the nucleon, x is the Bjorken variable, $D_{\Lambda^0/q}(z)$ is the probability for a quark of flavour q to fragment into a Λ^0 hyperon and z is the fraction of the quark energy carried by the produced Λ^0. The polarized fragmentation functions $\Delta D_{\Lambda/q}(z)$ are defined as

$$\Delta D_{\Lambda^0/q}(z) = D_{q^\uparrow}^{\Lambda^\uparrow}(z) - D_{q^\uparrow}^{\Lambda^\downarrow}(z), \tag{2}$$

where $D_{q^\uparrow}^{\Lambda^{\uparrow(\downarrow)}}(z)$ is the probability for a positively polarized quark to fragment in a positively (negatively) polarized Λ^0. The term $\hat{A}_{LL}(y)$, where y is the fraction of the incoming beam energy carried by the exchanged virtual photon, accounts for the elementary dynamics of the lepton-photon vertex and is given by

$$\hat{A}_{LL}(y) = \frac{y(2-y)}{1+(1-y)^2}. \tag{3}$$

This term grows from $\hat{A}_{LL} = 0$ for $y = 0$ to $\hat{A}_{LL} = 1$ for $y = 1$, and therefore $P^{(+,0)}(x, y, z)$ is a growing function of y. The underlaying dynamics of the fragmentation process and polarization transfer are non-perturbative, and some phenomenological models have to be considered.

In the non-relativistic quark model the spin of the Λ^0 is entirely carried by its constituent s quark. Therefore the polarization transfer from the initial lepton to the directly produced Λ^0 occurs in the fragmentation of the s quark only. A more refined approach[6] has been applied in[7] to the polarized lepton DIS process. The contribution of the fragmentation of u and d quarks to the polarization of the directly produced Λ^0's has been estimated. The calculations show that this contribution is of the order of 20% and has an opposite sign with respect to the polarization induced by the s quark fragmentation. The numerical estimates of the expected Λ^0 longitudinal polarization have been performed under conditions similar to that of the COMPASS experiment, assuming a beam of longitudinally polarized muons with an energy of 200 GeV and a polarization of $P_\mu = -80\%$, $Q^2 > 4$ GeV^2, $x_F > 0$ and $z > 0.2$, where x_F is the Feynman x variable and z is the fraction of the fragmenting quark momentum carried by the Λ^0 hyperon. The predicted longitudinal polarization of Λ^0 is $P_\Lambda = -0.12$ for the non-relativistic quark model and $P_\Lambda = -0.02$ for the model of[6]. The corresponding predictions for $\overline{\Lambda^0}$ are $P_{\overline{\Lambda}} = -0.14$ and $P_{\overline{\Lambda}} = -0.05$ respectively.

2   The experimental apparatus

In the COMPASS experiment[8] (see Fig. 1) a polarized muon beam ($E_\mu = 160$ GeV, $P_\mu = -76\%$) hits a polarized target system ($P_T \simeq 50\%$), that contains two 60 cm long ^{6}LiD cells polarized in opposite directions. The target polarization can be oriented either longitudinally or transversely with respect to the beam direction. The data presented in this paper refer to the longitudinal target polarization. The events from each target cell have been combined togheter and averaged over the two longitudinal orientations, therefore the effective target was unpolarized.

Reaction products are detected by a two-stage spectrometer with complementary kinematical acceptances: the Large Angle Spectrometer (LAS) has acceptance for particles emitted at low momenta or large angles, while the Small Angle Spectrometer (SAS) reconstructs high momentum particles. Each
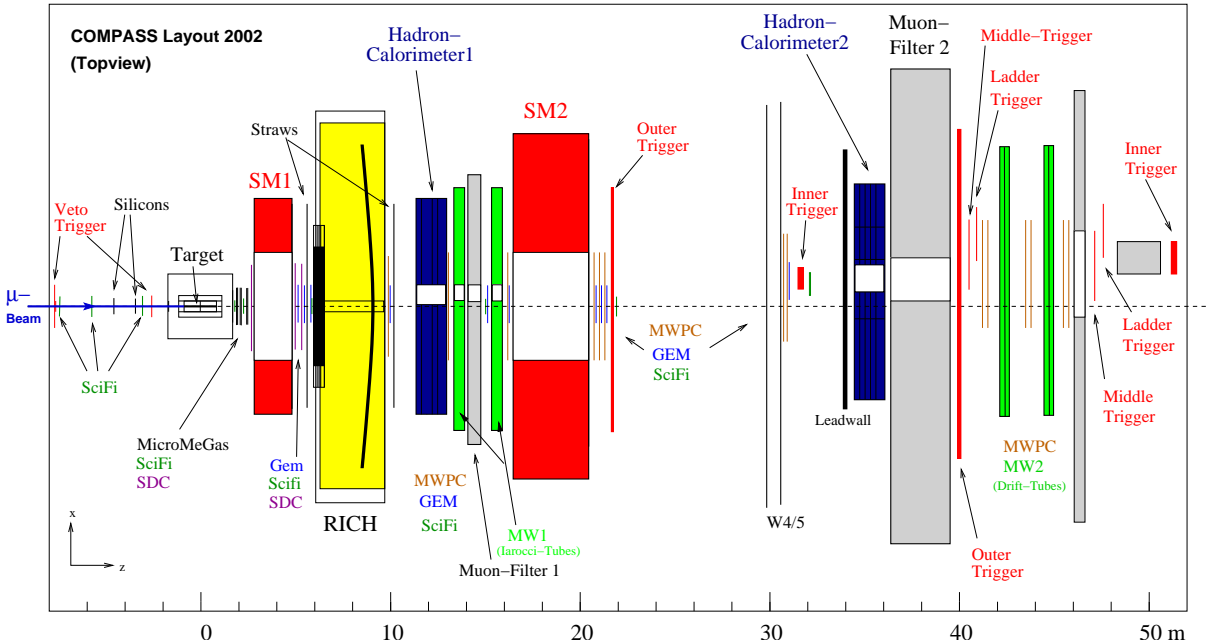

Figure 1: *Schematic view of the COMPASS 2002 setup.*

spectrometer stage is equipped with a dipole magnet, tracking detectors for momentum determination and particle identification devices.

Small area silicon and scintillating fiber detectors, providing a high spatial and time resolution, cover the region close to the beam axis, where the particle flux is maximal. The intermediate region is covered by micropattern gaseous detectors, while the particles at large angles and small momentum are tracked using drift chambers and multiwire proportional chambers. Most of the detectors are equipped with dead zones in the area where the particle flux is too high for their characteristics, the dead zone being covered by the trackers with smaller area and higher flux capablities.

Beam particles upstream of the polarized target are tracked by a combined system of scintillating fiber detectors and silicon microstrip detectors.

The LAS is located just downstream of the polarized target and has an acceptance of ±180 mrad. The LAS dipole magnet (SM1) is characterized by a field of 1 Tm and momentum acceptance for particles up to 60 GeV/c. Tracking of particles close to the beam is performed by means of scintillating fiber detectors, MicroMegas detectors upstream of SM1 and Gas Electron Multiplier (GEM) detectors downstream of it. The tracking of particles at larger angles is performed with Drift Chamber (DC) and straw detectors. The RICH1 Cherenkov detector separates pions and kaons up to momenta of 40 GeV/c. Muon identification in the LAS is provided by Iarocci-like chambers (MW1), made of 8 cells elements tracking particles crossing a thick iron absorber, stopping all the hadrons.

The SAS provides acceptance for particles with momenta higher than 10 GeV/c. The dipole magnet (SM2) has a field of 4.4 Tm. Tracking of beam particles is again performed with scintillating fiber detectors, while the remaining particles are tracked with a combined system of MultiWire Proportional Chambers(MWPC) for the outer region and GEM detectors for the region closer to the beam. Muon dentification in the SAS is provided by MWPC and aluminium drift tube chambers, tracking particles downstream an hadron absorber.

2.1 The trigger system

The 160 GeV muon beam used in COMPASS is characterized by a significant amount of halo, which represents a background for the detection of muons scattered from the polarized target. The COMPASS trigger system has therefore been designed to select the interactions in the target and reject halo particles. Several hodoscopes provide the coverage of a range in the four momentum transfer Q^2 from 10^{-4} to $30\,\mathrm{GeV}^2$ and for x from 10^{-5} to 1. The trigger logic processes the hodoscope information to select muons pointing to the target and reject beam halo contaminations. Several trigger types covering different regions of Q^2 and x (see Fig. 2) compete in the definition of the experiment's trigger.

3 Measurement of Λ^0 and $\overline{\Lambda^0}$ polarization

3.1 Selection of the sample

The Λ^0 and $\overline{\Lambda^0}$ are identified from their weak decay modes $\Lambda^0 \to p\pi^-$ and $\overline{\Lambda^0} \to \overline{p}\pi^+$, that occur with a branching ratio of $\sim 64\%$. The signature of such decays is the emission of two particles with opposite charges. The Λ^0 and $\overline{\Lambda^0}$ hyperons cannot decay by strong interactions, due to the strangeness quantum number conservation, and therefore are characterized by quite large lifetimes which, at the typical energies of COMPASS, allow to separate the production and decay vertices.

The production vertex, determined with a typical resolution of ~ 1 cm in the beam direction and of ~ 1 mm in the transverse direction, is required to be contained in one of the two target cells, while the decay vertex must be outside of the target volume. This requirement introduces a minimum distance of 5 cm between the production and decay vertices and avoids the interaction of the decay products with the target material, thus improving the invariant mass resolution and significantly reducing the background. A cut on the minimum transverse momentum $p_T > 23$ MeV/c of the positive decay particle with respect to the Λ^0 direction is also applied to reduce the background due to electron-positron pairs. Particles at the limits of the COMPASS acceptance are rejected by requiring a momentum $p > 1$ GeV/c.
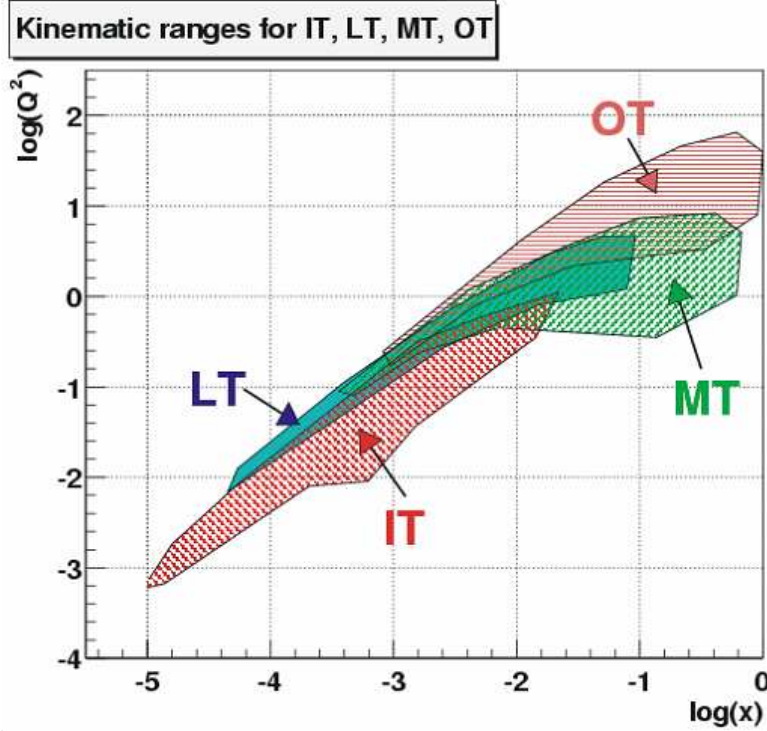
Figure 2: *COMPASS triggers.*

The deep inelastic scattering region is selected by requiring the squared four momentum transferred by the virtual photon to be $Q^2 > 1$ GeV^2. The cut $0.2 < y < 0.9$ is also applied to assure a mean photon depolarization $\hat{A}_{LL}(y)$ of 0.4.

The invariant mass of the sample passing all the selection cuts is shown in Fig. 3 for the three hypothesis of $K^0 \to \pi^+\pi^-$, $\Lambda^0 \to p\pi^-$ and $\overline{\Lambda^0} \to \pi + \overline{p}$ decays respectively. The sample shown refers to $\sim 1/6$ of the total 2002 statistics. The invariant masses have been fitted with a gaussian distribution plus a 3-rd degree polynomial for the background, and the number of K_s^0, Λ^0 and $\overline{\Lambda^0}$ has been calculated from the area of the gaussian peak. It is worth noting that the ratio between the number of Λ^0 and $\overline{\Lambda^0}$ is approximately 2/1: the large statistics of reconstructed $\overline{\Lambda^0}$ events is one of the advantages of the COMPASS experiment.

3.2 Extraction of the polarization

The Λ^0 polarization is extracted from the angular distribution of the decay products in the hyperon rest frame. Let's first of all introduce the momentum vectors of the exchanged virtual photon (p_{γ^*}) and of the target nucleon (p_{p^*}), taken in the rest frame of the Λ^0. Three orthogonal polarization axes are defined from this two vectors: the x axis (longitudinal) coincides with p_{γ^*}, the y axis (transversal) coincides with the normal to the production plane, defined as $p_{\gamma^*} \times p_{p^*}/|p_{\gamma^*} \times p_{p^*}|$. Finally the z axis (sideway) is defined as $z = x \times y$.

The theoretical angular distribution of the positive decay particle along the i-th direction (where i can be either x, y or z) is given by

$$N(\cos\theta_i^*) = \frac{N_{tot}}{2}(1 + \alpha P_i \, \cos(\theta_i^*)) \quad \text{for } \Lambda^0 \text{ decays,} \tag{4}$$

$$N(\cos\theta_i^*) = \frac{N_{tot}}{2}(1 - \alpha P_i \, \cos(\theta_i^*)) \quad \text{for } \overline{\Lambda^0} \text{ decays,} \tag{5}$$
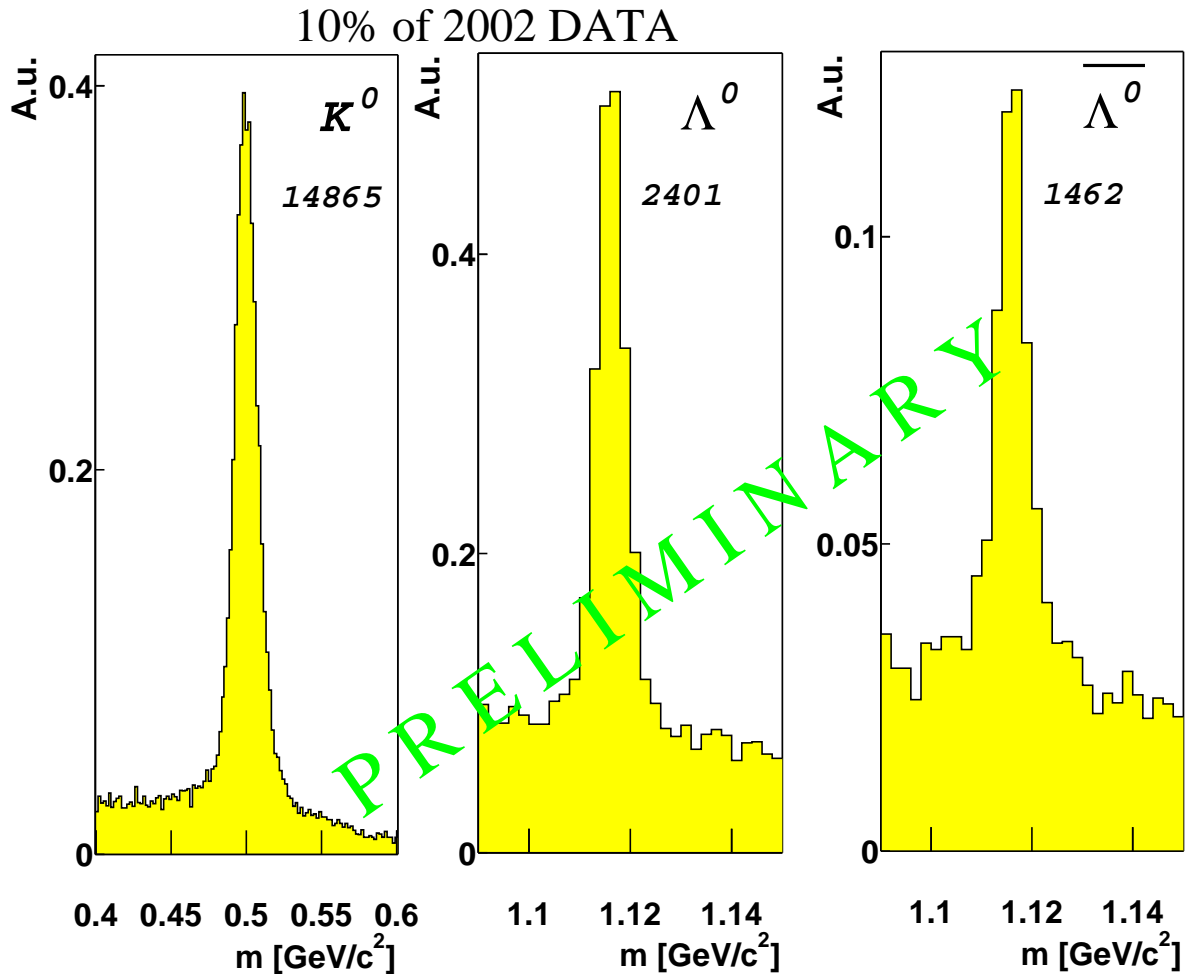
4

Figure 3: *Invariant mass distribution of events after all the selection cuts, for the three hypotheses of $K^0 \to \pi^+\pi^-$, $\Lambda^0 \to p\pi^-$ and $\overline{\Lambda^0} \to \pi + \overline{p}$ decays respectively. The statistics given in the figure for each species refers to the analysis of $\sim 10\%$ of the data collected in the year 2002.*

where θ_i^* is the angle between the momentum vector of the positive decay hadron and the i-th axis, computed in the rest frame of the decaying hyperon. P_i is the (unknown) polarization value, $\alpha = 0.642 \pm 0.013$ is the asymmetry parameter in the weak decay, and N_0 is the total number of events in the sample.

The experimental distributions $N_{exp}(\cos\theta_i^*)$ are in general distorted by the acceptance of the apparatus $A(\cos\theta_i^*)$ which is also function of the decay angle θ_i^*. The "true" angular distribution is therefore given by

$$N(\cos\theta_i^*) = \frac{N_{exp}(\cos\theta_i^*)}{A(\cos\theta_i^*)}. \tag{6}$$

A complete simulation of the COMPASS apparatus, based on the LEPTO 6.5.1[9] program for the DIS process, and the COMGEANT[10] and CORAL[11] programs for detector simulation and event reconstruction respectively, has been performed to evaluate and correct for the acceptance function $A(\cos\theta_i^*)$. No polarization of the Λ^0 hyperons has been introduced in the simulation. The level of agreement between the real data and the Monte Carlo simulation for some of the kinematical variables of interest is

shown in Figs. 4–5. Most experimental distributions are well reproduced by the Monte Carlo simulation.

The experimental data have been divided into 10 bins in $\cos(\theta_i^*)$ and the invariant mass in each bin has been fitted to extract the number of neutral decays and subtract the background. No binning in kinematical variables has been applied so far. The acceptance corrected experimental distributions are shown in Fig. 6 for the hypothesis of (from top to bottom) $K^0 \to \pi^+\pi^-$, $\Lambda^0 \to p\pi^-$ and $\overline{\Lambda^0} \to \pi + \overline{p}$ decays. The first column shows the overall invariant mass distribution of the sample used in the determination of the angular distributions, while the other three columns contain the corrected angular distributions along the longitudinal (x), transversal (y) and sideway (z) directions respectively.

In the case of the K^0 hypothesis all three distributions are flat, as it is expected for a spin zero particle. All the angular distributions are consistent with the small value of Lambda and anti-Lambda polarisation.

4   Conclusions

The preliminary results on Λ^0 and $\overline{\Lambda^0}$ analysis from the 2002 run of the COMPASS experiment have been presented. The available statistics in the kinematical region $Q^2 > 1$ GeV^2 and $0.2 < y < 0.9$ resulting from the analysis of $\sim 1/6$ of the 2002 data is ~ 3600 Λ^0's and ~ 2000 $\overline{\Lambda^0}$'s. This gives good perspectives for the precise measurement of the polarization transfer from the longitudinally polarized muon beam to the final state hyperons using full statistics.

We have measured the angular distributions of the positive decay particle in the hyperon helicity frame, correcting the apparatus accetance with MonteCarlo simulations. All acceptance-corrected angular distributions are rather flat, which means that polarization effects are small.

A fraction of $\sim 20\%$ of the 2002 data has also been taken with a trasversely polarized target. The expected Λ^0 and $\overline{\Lambda^0}$ statistics is comparable to that presented in this paper and would allow a first measurement of the polarization transfer from a transversely polarized target to the Λ^0 and $\overline{\Lambda^0}$ hyperons, that is directly related to the transverse spin distributions of the quarks in the nucleon.

References

[1] M. Anselmino, A. Efremov, E. Leader, Phys. Rep. **261** (1995) 1;
    R. Windmolders, Nucl. Phys. **B**, Proc. Suppl. **79** (1999) 51;
    B.W. Filippone and X. Ji, Adv. Nucl. Phys. **26** (2001) 1, e-Print Archive: hep-ph/0101224

[2] J. Ellis, D. Kharzeev, A.M. Kotzinian, Z. Physik **C69** (1996) 467

[3] J. Ellis, A.M. Kotzinian, D.V. Naumonov, Eur. Phys. J. **C25** (2002) 603

[4] P. Astier *et al.*, Nucl. Phys. **B588** (2000) 3; P. Astier *et al.*, Nucl. Phys. **B605** (2001) 3

[5] M. Anselmino, M. Boglione, F. Murgia, Phys. Lett **B481** (2000) 253

[6] M. Burkardt, R.L. Jaffe, Phys. Rev. Lett. **70** (1993) 2537

[7] A.M. Kotzinian, A. Bravar, D. von Harrach, Eur. Phys. J. **C2** (1998) 329

[8] CERN/SPSLC 96-14, SPSLC/P297, 1996.

[9] G. Ingelman, A. Edin, J. Rathsman, Comp. Phys. Comm. **101** (1997) 108

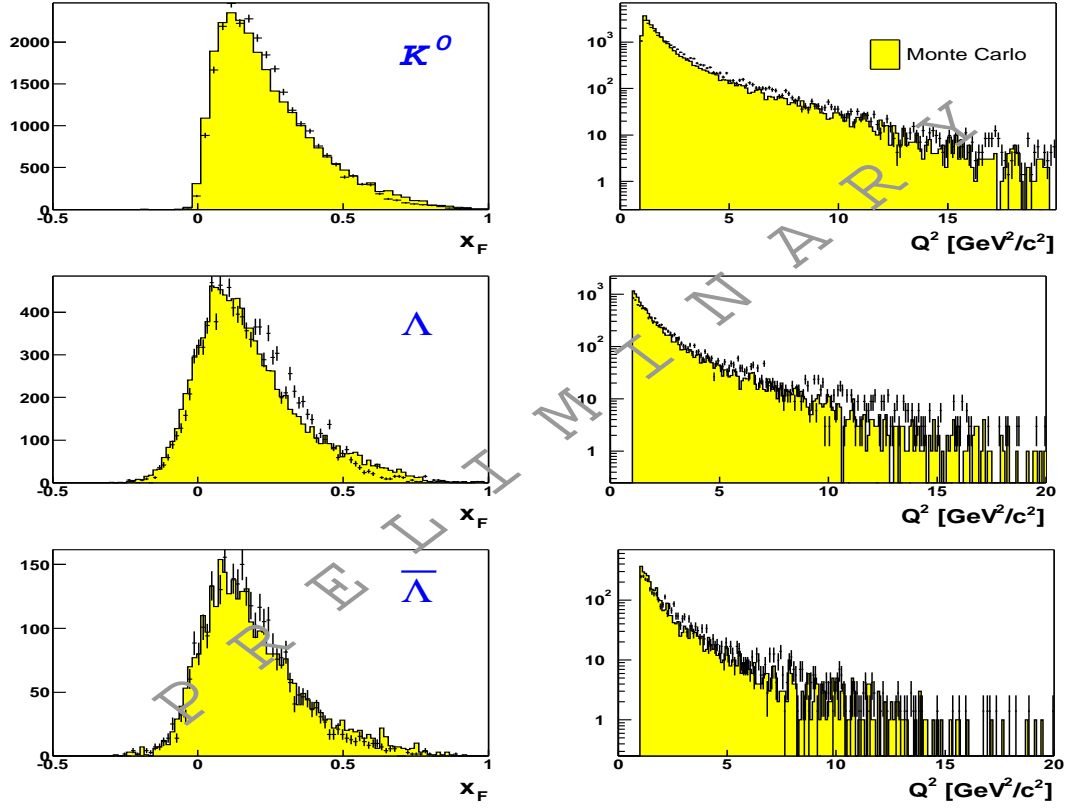[10] http://valexakh.home.cern.ch/valexakh/wwwcomg/index.html

[11] http://coral.web.cern.ch/coral/

Figure 4: x_F and Q^2 distributions of events compatible with, from top to bottom, K_s^0, Λ^0 and $\overline{\Lambda^0}$ hypotheis. The points with error bars correspond to real data, the filled area to the MonteCarlo simulation.
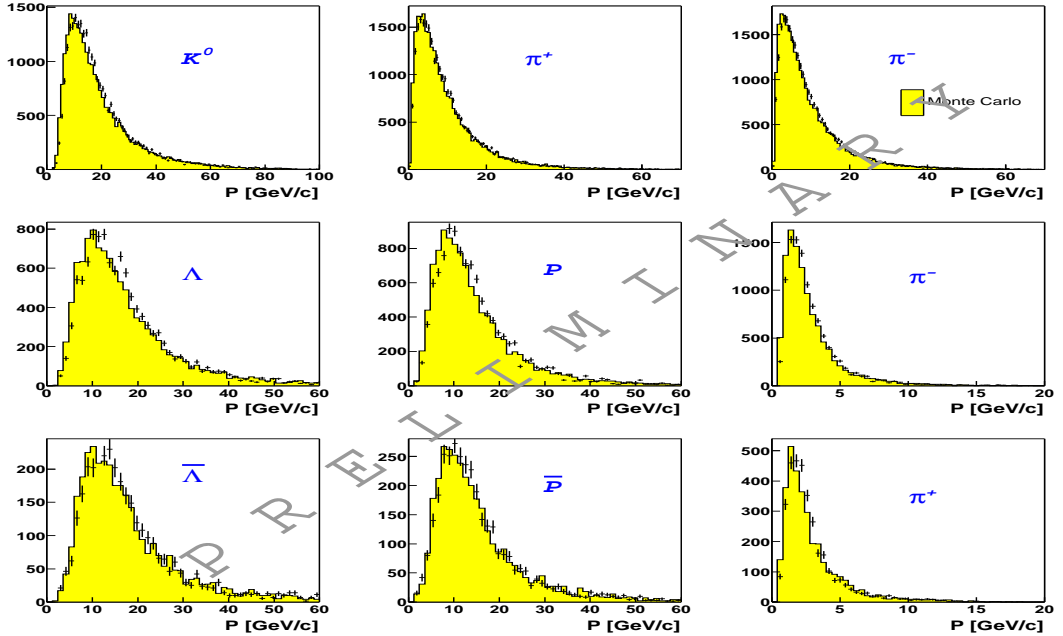

Figure 5: Momentum distributions for the strange particles and their decay products. The points with error bars correspond to real data, the filled area to the MonteCarlo simulation.
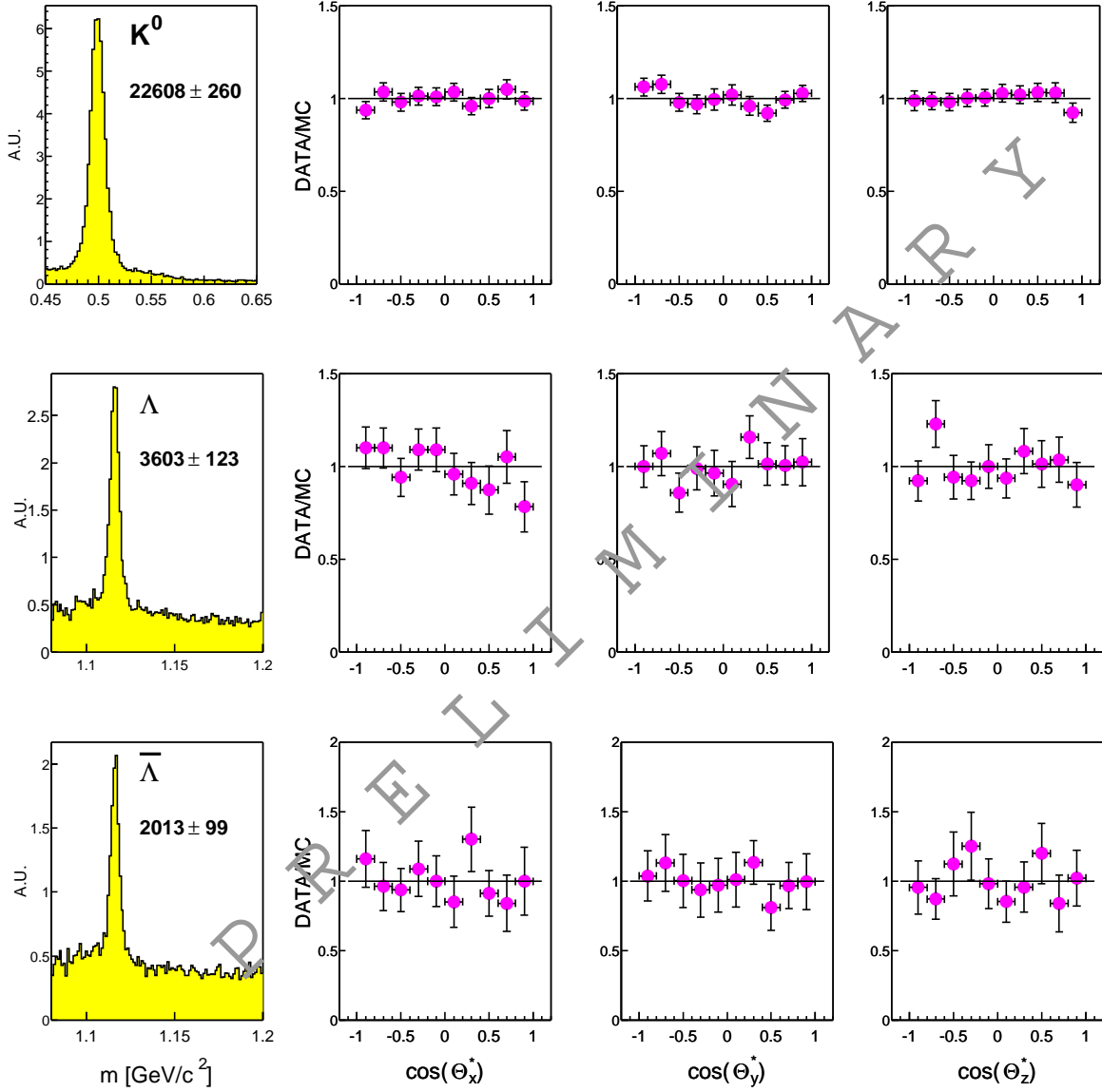
Figure 6: *Corrected* $\cos(\theta_x^*)$ *(second column)*, $\cos(\theta_y^*)$ *(third column)*, $\cos(\theta_z^*)$ *(forth column) in the hypothesis of (from top to bottom)* $K^0 \to \pi^+\pi^-$, $\Lambda^0 \to p\pi^-$ *and* $\overline{\Lambda^0} \to \pi + \overline{p}$ *decays. The first column shows the invariant mass distribution for all events for the three mass hypotheses.*